Hidden charge-2*e* boson: Experimental consequences for doped Mott insulators

Ting-Pong Choy,[1,2] Robert G. Leigh,[1] and Philip Phillips[1,2]
[1]*Department of Physics, University of Illinois, 1110 West Green Street, Urbana, Illinois 61801, USA*
[2]*Kavli Institute for Theoretical Physics, University of California, Santa Barbara, California 93106-4030, USA*
(Received 19 December 2007; published 25 March 2008)

We show here that many of the normal state properties of the cuprates can result from the new charge 2*e* bosonic field which we have recently [Phys. Rev. Lett. **99**, 046404 (2007); Phys. Rev. B **77**, 014512 (2007)] shown to exist in the exact low-energy theory of a doped Mott insulator. In particular, the (1) midinfrared band including the nonvanishing of the restricted *f*-sum rule in the Mott insulator, (2) T^2 contribution to the thermal conductivity, (3) pseudogap, (4) bifurcation of the electron spectrum below the chemical potential, as recently seen in angle-resolved photoemission, (5) insulating behavior away from half-filling, (6) high- and low-energy kinks in the electron dispersion, and (7) *T*-linear resistivity all derive from the charge 2*e* bosonic field. We also calculate the inverse dielectric function and show that it possesses a sharp quasiparticle peak and a broad particle-hole continuum. The sharp peak is mediated by a new charge *e* composite excitation formed from the binding of a charge 2*e* boson and a hole and represents a distinctly new prediction of this theory. It is this feature that is responsible for the dynamical part of the spectral weight transferred across the Mott gap. We propose that electron-energy loss spectroscopy at finite momentum and frequency can be used to probe the existence of such a sharp feature.

DOI: 10.1103/PhysRevB.77.104524 PACS number(s): 74.70.−b

I. INTRODUCTION

Key challenges facing a theory of the normal state (at zero magnetic field) of the copper oxide high temperature superconductors include the (1) *T*-linear resistivity,[1] (2) pseudogap,[2,3,5] (3) absence of quasiparticles,[4] and (4) midinfrared band in the optical conductivity.[6–11] Since the parent cuprates are Mott insulators, the normal state properties should, in principle, be derivable from the corresponding low-energy theory. Proper low-energy theories are constructed by integrating out the degrees of freedom far away from the chemical potential.

While no shortage of low-energy theories has been proposed,[12–29,33] none, until recently,[30,31] has been based on an explicit integration of the degrees of freedom at high energy even in the simplest model for a doped Mott insulator,

$$H_{\mathrm{Hubb}} = -t\sum_{i,j,\sigma} g_{ij} c^{\dagger}_{i,\sigma} c_{j,\sigma} + U\sum_{i,\sigma} c^{\dagger}_{i,\uparrow} c^{\dagger}_{i,\downarrow} c_{i,\downarrow} c_{i,\uparrow}. \tag{1}$$

Here, i,j label lattice sites, g_{ij} is equal to 1 if and only if i,j are nearest neighbors, $c_{i\sigma}$ annihilates an electron with spin σ on lattice site i, t is the nearest-neighbor hopping matrix element and U is the energy cost when two electrons doubly occupy the same site. The cuprates live in the strongly coupled regime in which the interactions dominate as $t \approx 0.5$ eV and $U=4$ eV. As U is the largest energy scale, it is appropriate to integrate over the fields that generate the physics on the U scale. We showed[30,31] explicitly how to perform such an integration. The corresponding low-energy theory contains degrees of freedom, namely, a charge 2*e* boson, (1) that are not in the original model and, more importantly, (2) that are not made out of the elemental excitations. We show here that this new degree of freedom mediates many of the anomalies in the normal state of the cuprates as probed by electrical and thermal transport as well as angular-resolved photoemission spectroscopy.

II. OVERVIEW OF LOW-ENERGY THEORY

In a series of papers,[30,31] we showed how to coarse grain the Hubbard model cleanly for $U \gg t$. We accomplished this by extending the Hilbert space of the Hubbard model and associating with the high-energy scale a new fermionic oscillator which is constrained. The coupling constant for the fermionic oscillator is U. We showed that once the constraint is solved, we obtained exactly the Hubbard model. However, since the energy scale of the new oscillator is U, the low-energy theory is obtained by integrating over this field. We showed explicitly[30,31] that the Lagrangian in the extended Hilbert space is quadratic in the high-energy field, and hence all integrals can be performed exactly. Let us define

$$\mathcal{M}_{ij} = \delta_{ij} - \frac{t}{(\omega + U)} g_{ij} \sum_{\sigma} c^{\dagger}_{j,\sigma} c_{i,\sigma} \tag{2}$$

and $b_i = \Sigma_j b_{ij} = \Sigma_{j\sigma} g_{ij} c_{j,\sigma} V_{\sigma} c_{i,-\sigma}$ with $V_{\uparrow} = -V_{\downarrow} = 1$. At zero frequency, the exact low-energy Hamiltonian is

$$H_h^{IR} = -t\sum_{i,j,\sigma} g_{ij} \alpha_{ij\sigma} c^{\dagger}_{i,\sigma} c_{j,\sigma} + H_{\mathrm{int}} - \frac{1}{\beta} \mathrm{Tr} \ln \mathcal{M},$$

where

$$H_{\mathrm{int}} = -\frac{t^2}{U}\sum_{j,k} b^{\dagger}_j (\mathcal{M}^{-1})_{jk} b_k - \frac{t^2}{U}\sum_{i,j} \varphi^{\dagger}_i (\mathcal{M}^{-1})_{ij} \varphi_j - t\sum_j \varphi^{\dagger}_j c_{j,\uparrow} c_{j,\downarrow} - \frac{t^2}{U}\sum_{i,j} \varphi^{\dagger}_i (\mathcal{M}^{-1})_{ij} b_j + \mathrm{H.c.}, \tag{3}$$

which contains a charge 2*e* bosonic field φ_i.

The low-energy theory acts only in the original Hilbert space of the Hubbard model because we integrated out all operators which acted in the extended space. Consequently, it is incorrect to interpret φ_i as a canonical boson operator with an associated Fock space. Likewise, we should not immedi-

ately conclude that φ_i gives rise to a propagating charge $2e$ bosonic mode, as it does not have canonical kinetics; at the earliest, this could be generated at order $O(t^3/U^2)$ in perturbation theory. Alternatively, we believe that φ appears as a bound degree of freedom. The new composite charge e state is crucial in explaining the origin of the dynamical spectral weight transfer across the Mott gap. As a consequence, the conserved charge is no longer just the electron number but rather

$$Q = \sum_{i\sigma} c_{i\sigma}^{\dagger} c_{i\sigma} + 2\sum_{i} \varphi_i^{\dagger}\varphi_i. \tag{4}$$

The terms containing φ_i are absent from projective theories and represent the fact that consistent with the Hubbard model, the corresponding low-energy theory is not diagonal in any sector containing a fixed number of doubly occupied sites. As we have shown elsewhere,[35] the presence of double occupancy in the low-energy theory presented above is completely compatible with the standard derivation of the t-J model. One simply has to remember that the operators appearing in the t-J model are transformed[32–34] fermions which are related by a similarity transformation to the bare electrons appearing in the Hubbard model. If the rotated fermions are expressed[35] in terms of the original electron operators in the Hubbard model, double occupancy of the bare fermions is reinstated. In fact, the t-J model expressed[35] in terms of the original bare electron operators contains processes which mix the doubly and singly occupied sectors with a matrix element t^2/U as in Eq. (3). However, it is common to interpret[12–29] the t-J model as a model of physically doped holes in a Mott insulator. Unless the operators in the t-J model are transformed back to the original basis, it is impossible to make any connection between doped holes in the two theories.

Physical processes mediated by the boson include singlet motion [third term in Eq. (3)] and motion of double occupancy in the lower-Hubbard band [second term in Eq. (3)]. The latter has a bandwidth of t and, as we will show, constitutes the midinfrared band. Since Eq. (3) retains all the low-energy degrees of freedom, a t/U expansion is warranted. To leading order in t/U, $\mathcal{M}=\delta_{ij}$, and the effective low-energy Hamiltonian simplifies to

$$H_{\text{eff}} = -t\sum_{i,j,\sigma} g_{ij}\alpha_{ij\sigma} c_{i,\sigma}^{\dagger} c_{j,\sigma} - \frac{t^2}{U}\sum_{j} b_j^{\dagger} b_j - \frac{t^2}{U}\sum_{i,j} \varphi_i^{\dagger}\varphi_i$$
$$- t\sum_{j} \varphi_j^{\dagger} c_{j,\uparrow} c_{j,\downarrow} - \frac{t^2}{U}\sum_{i,j} \varphi_i^{\dagger} b_i + \text{H.c.} \tag{5}$$

The first two terms contain the interactions in the t-J model as the two-site term in $b_j^{\dagger} b_j$ is proportional to the unprojected spin-spin interaction. In second-order perturbation theory, the interaction term $\varphi_i^{\dagger} b_i$ mediates the process in Fig. 1. In this process, hole motion over three sites is possible only if a doubly occupied site and a hole are neighbors. This process is absent if one assumes that the no-double occupancy condition in the t-J model applies to the bare electrons as well. The latter is true exactly at $U=\infty$. As we will see, this process, which is present as a result of the bosonic degree of freedom, is responsible for many of the anomalous properties of the normal state of the cuprates.

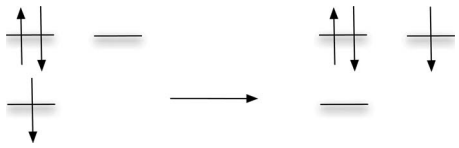

FIG. 1. Hopping processes mediated by the φ_i operator in the low-energy theory obtained by explicitly integrating out the high-energy sector. This process is in the t-J model only if one transforms the electron operators back to the original Hubbard basis, retaining the terms that change the number of doubly occupied sites.

A. Electron spectral function

We analyze the nature of the electronic excitations at low energy by focusing on the electron spectral function. Since this calculation cannot be done exactly, we establish at the outset the basic physics that a correct calculation should preserve. We have shown previously[30,31] that the electron creation operator at low energy,

$$c_{i,\sigma}^{\dagger} \to (1-n_{i,-\sigma}) c_{i,\sigma}^{\dagger} + V_{\sigma}\frac{t}{U} b_i^{\dagger} \mathcal{M}_{ij}^{-1} c_{j,-\sigma} - V_{\sigma}\frac{s}{U}\varphi_i^{\dagger}\mathcal{M}_{ij}^{-1} c_{j,-\sigma}, \tag{6}$$

contains the standard term for motion in the lower Hubbard band (LHB), $(1-n_{i,-\sigma})c_{i,\sigma}^{\dagger}$ [$n_{i,-\sigma}c_{i\sigma}$ in the upper Hubbard band (UHB) for electron doping] with a renormalization from spin fluctuations (second term) and a new charge e excitation, $c_{i,-\sigma}\mathcal{M}_{ij}^{-1}\varphi_j^{\dagger}$. In the lowest order in t/U, our theory predicts that the new excitation corresponds to $c_{i,-\sigma}\varphi_i^{\dagger}$, that is, a hole bound to the charge $2e$ boson. This extra charge e state mediates the dynamical (hopping-dependent) spectral weight transfer across the Mott gap.

Consequently, we predict that an electron at low energies is in a superposition of the standard LHB state (modified with spin fluctuations) and a new charge e state which is a composite excitation. It is the presence of these two distinct excitations that gives rise to the static (state counting giving rise to $2x$)[38] and dynamical parts of the spectral weight transfer. A saddle-point analysis will select a particular solution in which φ_i is nonzero. This will not be consistent with the general structure of Eq. (6) in which part of the electronic states are not fixed by φ_i. Similarly, mean-field theory in which φ_i is assumed to condense, thereby thwarting the possibility that new excitations will form, is also inadequate.

The procedure we adopt is the simplest that preserves the potential strong interactions between the Bose and Fermi degrees of freedom. We treat φ_i to be spatially independent with no dynamics of its own. This interpretation is consistent with the fact that φ_i acquires dynamics only through electron motion. Under this assumption, the single-particle electron Green function

$$G(k,\omega) = -i\text{FT}\langle T c_i(t) c_j^{\dagger}(0)\rangle \tag{7}$$

can be calculated rigorously in the path-integral formalism as

$$G(k,\omega) = -i\mathrm{FT}\int [D\varphi_i^*][D\varphi_i]\int [Dc_i^*][Dc_i]c_i(t)c_j^*(0) \times \exp\left(-\int L[c,\varphi]dt\right), \tag{8}$$

where FT refers to the Fourier transform and **T** is the time-ordering operation. Further, since our focus is on the new physics mediated by the interaction between the Bose and Fermi degrees of freedom and Eq. (6) suggests that the spin-spin interaction simply renormalizes the electronic states in the LHB, we will neglect the spin-spin term. To see what purely fermionic model underlies the neglect of the spin-spin term in Eq. (5), we integrate over φ_i. The full details of how to carry out such an integration are detailed elsewhere.[31] The resultant Hamiltonian is not the Hubbard model but rather

$$H' = H_{\mathrm{Hubb}} - \frac{t^2}{U}\sum_i b_i^\dagger b_i, \tag{9}$$

a t-J-U model in which the spin-exchange interaction is not a free parameter but fixed to $J=-t^2/U$. That the t-J-U model with $J=-t^2/U$ is equivalent to a tractable IR model, namely, Eq. (5) without the spin-spin term, is an unexpected simplification. As Mott physics still pervades the t-J-U model in the vicinity of half-filling, our analysis should reveal the nontrivial charge dynamics of this model. That is, the physics we uncloak here is independent of the spin degrees of freedom. In fact, what we show is that the spin-spin interaction (as in the hard-projected t-J model) is at best ancillary to many of the normal state properties of the cuprates.

To proceed, we will organize the calculation of $G(k,\omega)$ by first integrating out the fermions (holding φ fixed),

$$G(k,\omega) = \int [D\varphi^*][D\varphi]\mathrm{FT}\left[\int [Dc_i^*][Dc_i]c_i(t)c_j^*(0) \times \exp\left(-\int L[c,\varphi]dt\right)\right], \tag{10}$$

where now

$$L = \sum_{i\sigma}(1-n_{i\bar{\sigma}})c_{k\sigma}^*\dot{c}_{k\sigma} - \left(2\mu + \frac{s^2}{U}\right)\varphi^*\varphi - \sum_{k\sigma}(g_t t\alpha_k + \mu)c_{k\sigma}^* c_{k\sigma} + s\varphi^*\sum_k\left(1-\frac{2t}{U}\right)c_{-k\downarrow}c_{k\uparrow} + \mathrm{c.c.} \tag{11}$$

The effective Lagrangian can be diagonalized and written as

$$L = \sum_{k\sigma}(1-n_{i\bar{\sigma}})\gamma_{k\sigma}^*\dot{\gamma}_{k\sigma} + \sum_k\left(E_0 + E_k - \lambda_k - \frac{2}{\beta}\ln(1+\exp^{-\beta\lambda_k})\right) + \sum_{k\sigma}\lambda_k\gamma_{k\sigma}^*\gamma_{k\sigma} \tag{12}$$

in terms of a set of Bogoliubov quasiparticles,

$$\gamma_{k\uparrow}^* = +\cos^2\theta_k c_{k\uparrow}^* + \sin^2\theta_k c_{-k\downarrow}, \tag{13}$$

$$\gamma_{k\downarrow} = -\sin^2\theta_k c_{k\uparrow}^* + \cos^2\theta_k c_{-k\downarrow}, \tag{14}$$

where $\cos^2\theta_k = \frac{1}{2}(1+\frac{E_k}{\lambda_k})$. Here, $\alpha_k = 2(\cos k_x + \cos k_y)$, $\eta_k = 2(\cos k_x - \cos k_y)$, $E_0 = -(2\mu + \frac{s^2}{U})\varphi^*\varphi$, $E_k = -g_t t\alpha_k - \mu$, $\lambda_k = \sqrt{E_k^2+\Delta_k^2}$, $\Delta_k = s\varphi^*(1-\frac{2t}{U}\alpha_k)$, and $g_t = \frac{2\delta}{1+\delta}$ when $\delta = 1-n \to 1-Q+2\varphi^*\varphi$ is a renormalized factor which originates from the correlated hopping term $(1-n_{i\bar{\sigma}})c_{i\sigma}^\dagger c_{j\sigma}(1-n_{j\bar{\sigma}})$. Starting from Eq. (12), we integrate over the fermions in Eq. (10) to obtain

$$G(k,\omega) = \frac{1}{Z}\int [D\varphi^*][D\varphi]G(k,\omega,\varphi) \times \exp\left\{-\sum_k\left[E_0 + E_k - \lambda_k - \frac{2}{\beta}\ln(1+\exp^{-\beta\lambda_k})\right]\right\}, \tag{15}$$

where

$$G(k,\omega,\varphi) = \frac{\sin^2\theta_k[\varphi]}{\omega+\lambda_k[\varphi]} + \frac{\cos^2\theta_k[\varphi]}{\omega-\lambda_k[\varphi]} \tag{16}$$

is the exact Green function corresponding to the Lagrangian, Eq. (12). The two-pole structure of $G(k,\omega,\varphi)$ will figure prominently in the structure of the electron spectral function. To calculate $G(k,\omega)$, we numerically evaluated the remaining φ integral in Eq. (15). Since Eq. (15) is averaged over all values of φ, we have circumvented the problem inherent in mean-field or saddle-point analyses. Physically, Eq. (15) serves to mix (through the integration over φ) all subspaces with varying number of double occupancies into the low-energy theory. Hence, it should retain the full physics inherent in the bosonic degree of freedom.

The spectral function for $U=10t$ evaluated from Eq. (16) and displayed in Figs. 2 and 3 exhibits four key features. First, regardless of the doping, there is a low-energy kink in the electron dispersion. The enlarged region in Fig. 2(a) shows, in fact, that two kinks exist. The low-energy kink occurs at roughly $0.2t \approx 100$ meV. By treating the mass term for the boson as a variable parameter, we verified that the low-energy kink is determined by the bare mass. In the effective low-energy theory, the bare mass is t^2/U. This mass is independent of doping. Experimentally, the low-energy kink[36] is impervious to doping. Consequently, the boson offers a natural explanation for this effect that is distinct from the phonon mechanisms which have been proposed.[36]

Second, a high-energy kink appears at roughly $0.5t \approx 250$ meV, which closely resembles the experimental kink at 300 meV.[37] At sufficiently high doping [see Figs. 3(a) and 3(b)], the high-energy kink disappears.

Third, experimentally, the high-energy kink is accompanied by a splitting of the electron dispersion into two branches.[37] As is evident, this is precisely the behavior we find below the chemical potential. The energy difference between the two branches achieves a maximum at (0,0), as is seen experimentally. A computation of the spectral function at $U=20t$ and $n=0.9$ reveals that the dispersion as well as the

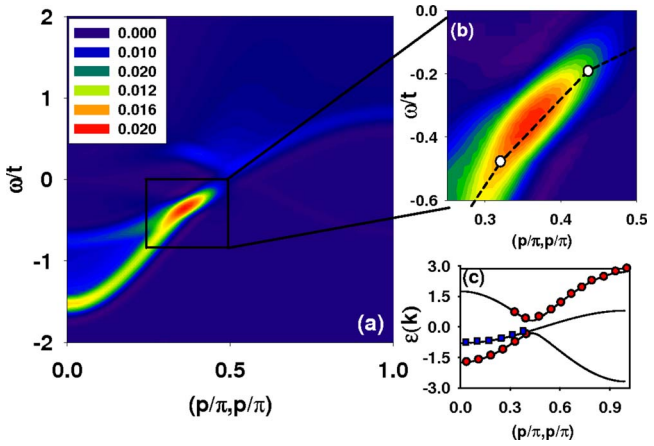

FIG. 2. (Color online) (a) Spectral function for filling $n=0.9$ along the nodal direction. The intensity is indicated by the color scheme. (b) Location of the low- and high-energy kinks as indicated by the change in the slope of the electron dispersion. (c) The energy bands that give rise to the bifurcation of the electron dispersion.

bifurcation still persist. Further, the magnitude of the splitting does not change, indicating that the energy scale for the bifurcation and the maximum energy splitting are set by t and not U. The origin of the two branches is captured in Fig. 2(c). The two branches below the chemical potential correspond to the standard band in the LHB [open square in Fig. 2(c)] on which φ vanishes and a branch on which $\varphi \neq 0$ [open circles in Fig. 2(c)]. The two branches indicate that there are two local maxima in the integrand in Eq. (15). One of the maxima, $\varphi=0$, arises from the extremum of $G(k,\omega,\varphi)$, whereas the other, the effective free energy [exponent in Eq. (15)], is minimized ($\varphi \neq 0$). Above the chemical potential, only one branch survives. The split electron dispersion below the chemical potential is consistent with the composite nature of the electron operator dictated by Eq. (6). At low energies, the electron is a linear superposition of two states, one the standard band in the LHB described by excitations of the form $c^{\dagger}_{i\sigma}(1-n_{i\bar{\sigma}})$ and the other a composite excitation consisting of a bound hole and the charge $2e$ boson, $c_{i\bar{\sigma}}\varphi^{\dagger}_{i}$. The former contributes to the static part of the spectral weight transfer ($2x$) while the new charge e excitation gives rise to the dynamical contribution to the spectral weight transfer. Because the new charge e state is strongly dependent on the hopping, it should disperse, as is evident from Fig. 3 and also confirmed experimentally.

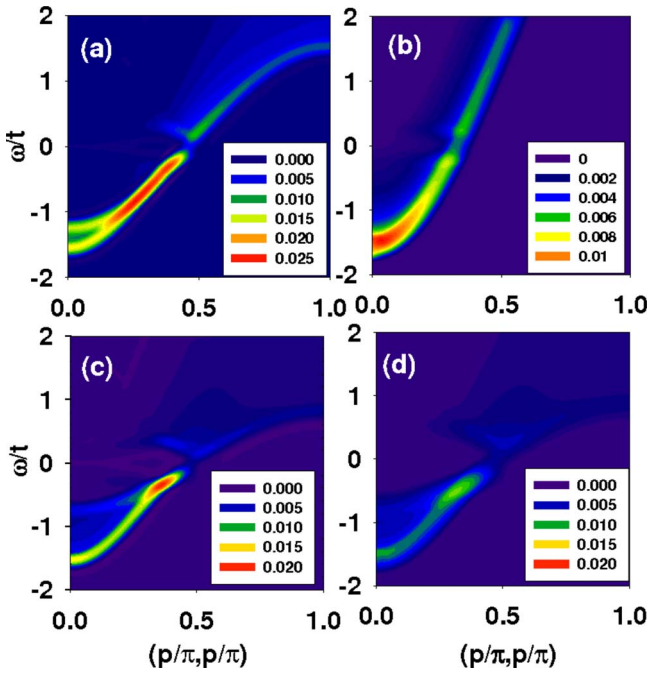

FIG. 3. (Color online) Spectral function for two different fillings, (a) $n=0.8$ and (b) $n=0.4$, along the nodal direction. The absence of a splitting in the electron dispersion at $n=0.4$ indicates that the bifurcation ceases beyond a critical doping. The spectral functions for two different values of the on-site repulsion, (c) $U=10t$ and (d) $U=20t$ for $n=0.9$, reveals that the high-energy kink and the splitting of the electron dispersion have at best a weak dependence on U. This indicates that this physics is set by the energy scale t rather than U.

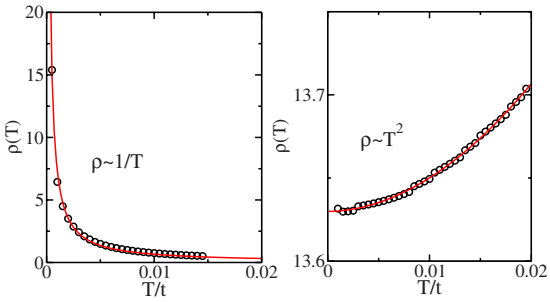

FIG. 4. (Color online) (a) dc electrical resistivity as a function of temperature for $n=0.9$. (b) Setting the bosonic degree of freedom to zero kills the divergence of the resistivity as $T \to 0$. This suggests that it is the strong binding between the fermionic and bosonic degrees of freedom that ultimately leads to the insulating behavior in the normal state of a doped Mott insulator.

The formation of the composite excitation, $c_{i\bar{\sigma}}\varphi^{\dagger}$, leads to a pseudogap at the chemical potential primarily because the charge $2e$ boson is a local nonpropagating degree of freedom. The spectral functions for $n=0.9$ and $n=0.8$ both show an absence of spectral weight at the chemical potential. Nonzero spectral weight resides at the chemical potential in the heavily overdoped regime, $n=0.4$, consistent with the vanishing of the pseudogap beyond a critical doping away from half-filling. Because the density of states vanishes at the chemical potential, we expect the electrical resistivity to diverge as $T \to 0$. Such a divergence is shown in Fig. 4(a) and is consistent with our previous calculations of the dc resistivity using a local dynamical cluster method.[39] When the boson is absent [Fig. 4(b)], localization ceases. Although this calculation does not constitute a proof, it is consistent with localization induced by the formation of the bound composite excitation, $c_{i\bar{\sigma}}\varphi^{\dagger}_{i}$. This state of affairs obtains because the boson is not an inherently dynamical excitation.

Finally, the imaginary part of the self-energy at different temperatures is shown in Fig. 5. At low temperature ($T \leqslant t^2/U$), the imaginary part of the self-energy at the noninteracting Fermi surface develops a peak at $\omega=0$. At $T=0$, the

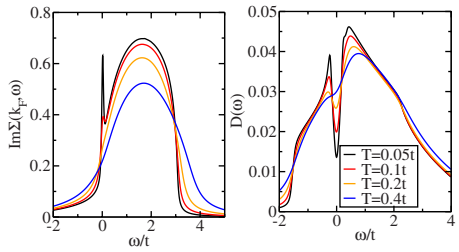

FIG. 5. (Color online) The imaginary part of the self-energy as a function of temperature for $n=0.7$. A peak is developed at $\omega=0$ at low temperature, which is the signature of the opening of the pseudogap. The density of states explicitly showing the pseudogap is shown in the adjacent figure.

peak leads to a divergence. This is consistent with the opening of a pseudogap. As we have pointed out earlier,[40] a pseudogap is properly identified by a zero surface (the Luttinger surface) of the single-particle Green function. This zero surface is expected to preserve the Luttinger volume if the pseudogap lacks particle-hole symmetry, as shown in the second of the figures in Fig. 5.

B. Midinfrared band

The midinfrared band (MIB) in the cuprates is a surprise because the optical conductivity in a doped Mott insulator is expected to be nonzero either at the far-infrared or the ultraviolet or the upper-Hubbard-band scale. While many mechanisms have been proposed,[11] no explanation has risen to the fore. Experimentally, the intensity in the MIB increases with doping at the expense of the spectral weight at high-energy, and the energy scale for the peak in the MIB is the hopping matrix element t. Since the MIB arises from the high-energy scale, the current theory which accurately integrates out the high-energy degrees of freedom should capture this physics. To obtain a direct link between the conductivity and the spectral function, we work in the noncrossing approximation,

$$\sigma_{xx}(\omega) = 2\pi e^2 \int d^2k \int d\omega' (2t \sin k_x)^2 \times \left(-\frac{f(\omega') - f(\omega'+\omega)}{\omega} \right) A(\omega+\omega',k) A(\omega',k), \tag{17}$$

to the Kubo formula for the conductivity, where $f(\omega)$ is the Fermi distribution function and $A(\omega,k)$ is the spectral function. At the level of theory constructed here, the vertex corrections are all due to the interactions with the bosonic degrees of freedom. Since the boson acquires dynamics only through electron motion and the leading such term is $O(t^3/U^2)$, the treatment here should suffice to provide the leading behavior of the optical conductivity.

The optical conductivity shown in Fig. 6 peaks at $\omega/t \approx 0.5t$, forming the MIB. As the inset indicates, $\omega_{\max}$ is an increasing function of electron filling (n), whereas the integrated weight

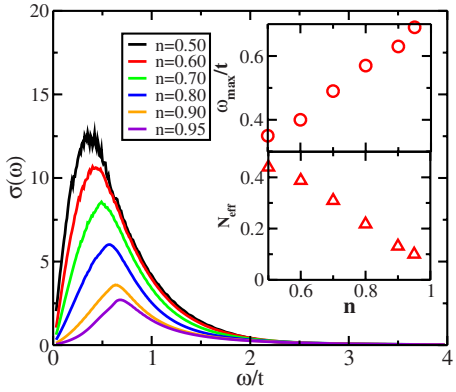

FIG. 6. (Color online) Optical conductivity as a function of electron filling n. The peak in the optical conductivity represents the midinfrared band. Its origin is mobile double occupancy in the lower-Hubbard band. The insets show that the energy at which the MIB acquires its maximum value, $\omega_{\max}$, is an increasing function of electron filling. Conversely, the integrated weight of the MIB decreases as the filling increases. This decrease is compensated with an increased weight at high (upper-Hubbard band) energy scale.

$$N_{\text{eff}} = \frac{2m^*}{\pi e^2} \int_0^{\Omega_c} d\sigma(\omega) \tag{18}$$

is a decreasing function. However, N_{eff} does not vanish at half-filling, indicating that the mechanism that causes the mid-IR is evident even in the Mott state. Here, we set the integration cutoff to $\Omega_c = 2t = 1/m^*$. Both the magnitude of $\Omega_{\max}$ and its doping dependence as well as the electron filling dependence of the integrated weight are consistent with those of the midinfrared band in the optical conductivity in the cuprates.[6,7,9–11] To determine what sets the scale for the MIB, we studied its evolution as a function of U. Figure 7 verifies that $\omega_{\max}$ is set essentially by the hopping matrix element t and depends only weakly on J. The physical processes that determine this physics are determined by the coupled boson-Fermi terms in the low-energy theory. The

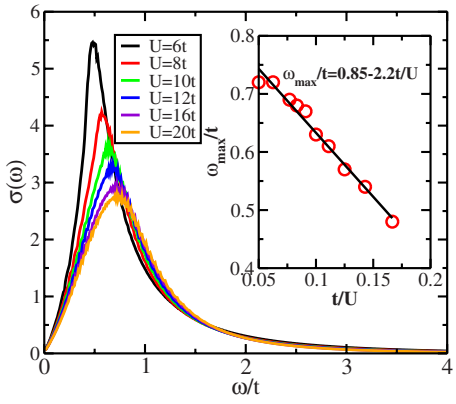

FIG. 7. (Color online) Evolution of the optical conductivity for $n=0.9$ as U is varied. The inset shows the functional form that best describes $\omega_{\max}$. The dominant energy scale is the hopping matrix element t since t/U for the cuprates is $O(1/10)$.

$\varphi_i^\dagger c_{i\uparrow} c_{i\downarrow}$ term has a coupling constant of t, whereas the $\varphi_i^\dagger b_i$ scales as t^2/U. Together, both terms give rise to a MIB that scales as $\omega_{\max}/t = 0.8 - 2.21 t/U$ (see inset of Fig. 7). Since $t/U \approx O(0.1)$ for the cuprates, the first term dominates and the MIB is determined predominantly by the hopping matrix element t. Within the interpretation that φ represents a bound state between a doubly occupied site and a hole, second-order perturbation theory with the $\varphi_i^\dagger b_i$ term mediates the process shown in Fig. 1. It is the resonance between these two states that results in the mid-IR band. Interestingly, this resonance persists even at half-filling, and hence the nonvanishing of N_{eff} at half-filling is not evidence that the cuprates are not doped Mott insulators, as has been recently claimed.[41] In their work, Comanac *et al.*[41] used a single-site dynamical mean-field approach. In such approaches, near-neighbor correlations are absent.

Since the physics in Fig. 1 is not present in projective models which prohibit double occupancy in the Hubbard basis (not simply the transformed fermion basis of the t-J model), it is instructive to see what the calculations of the optical conductivity in the t-J model reveal. All existing calculations[10,42,43] on the t-J model find that the MIB scales as J. In some of these calculations, superconductivity is needed to induce a MIB (Ref. 43) also at an energy scale of J. Experimentally,[6,7,11] it is clear that the MIB is set by the t scale rather than J. In fact, since the MIB grows at the expense of the spectral weight in the upper-Hubbard band, it is not surprising that the t-J model cannot describe this physics, as first pointed out by Uchida *et al.*[7] The physical mechanism we have identified here (Fig. 1 clearly derives from the high-energy scale) has the correct energy dependence, and hence satisfies the key experimental constraints on the origin of the MIB. Since the physics in Fig. 1 is crucial to the mid-IR, it is not surprising that single-site analyses[41] fail to obtain a nonzero intercept in the extreme Mott limit. The nonzero intercept of N_{eff} is a consequence of Mottness and appears to be seen experimentally in a wide range of cuprates.[6,44–46]

C. Dielectric function: Experimental prediction

In the previous section, we have calculated the electronic spectral function which shows that there are two branches below the chemical potential. Such physics is explained by the formation of a new composite excitation, representing a bound state, consisting of a bound hole and a charge $2e$ boson, $\varphi_i^\dagger c_{i\bar{\sigma}}$. We demonstrated that for the MIB in the optical conductivity, such an excitation also appears. In principle, these composite charge excitations should show up in all electric response functions, for example, the energy loss function, $\Im 1/\epsilon(\omega, \mathbf{q})$, where $\epsilon(\omega, \mathbf{q})$ is the dielectric function. We show here that this is the case.

To this end, we calculate the inverse dielectric function,

$$\Im \frac{1}{\epsilon(\omega, \mathbf{q})} = \pi \frac{U}{v} \sum_p \int d\omega' [f(\omega') - f(\omega + \omega')] \times A(\omega + \omega', \mathbf{p} + \mathbf{q}) A(\omega', \mathbf{p}), \quad (19)$$

using the noncrossing approximation discussed earlier. Our results are shown in Fig. 8 for $n = 0.9$ and $n = 0.6$ for $\mathbf{q}$ along the diagonal. Two features are distinct. First, there is a broad band (red arrow in Fig. 6) with the width of order t that disperses with $\mathbf{q}$ for both doping levels. It is simply the particle-hole continuum which arises from the bare electron band. The band width is doping dependent as a result of the renormalization of the band with doping. More strikingly, for $n = 0.9$, a sharp peak exists at $\omega/t \approx 0.2t$. It disperses with q, terminating when $\mathbf{q} \to (\pi, \pi)$. Physically, the sharp peak represents a quasiparticle excitation of the composite object, $\varphi_i^\dagger c_{i\bar{\sigma}}$, the charge $2e$ boson and a hole. Therefore, we predict that if this new composite charge excitation, $\varphi_i^\dagger c_{i\bar{\sigma}}$, is a real physical entity, as it seems to be, it will give rise to a sharp peak in addition to the particle-hole continuum in the inverse dielectric function. Since this function has not been measured at present, our work here represents a prediction. Electron-energy loss spectroscopy can be used to measure the inverse dielectric function. Our key prediction is that momentum-dependent scattering should reveal a sharp peak that appears at low energy in a doped Mott insulator. We have checked numerically the weight under the peaks in the inverse dielectric function and the sharp peak is important. Hence, the new charge e particle we have identified here should be experimentally observable.

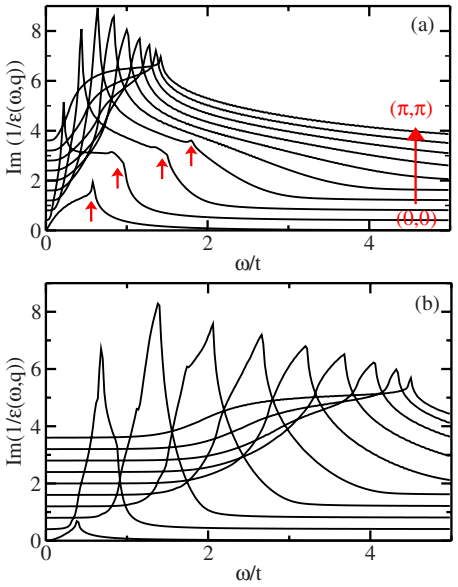

FIG. 8. (Color online) The dielectric function $-\Im 1/\epsilon(\omega, \mathbf{q})$ for $\mathbf{q}$ along the diagonal direction is shown for (a) $n = 0.9$ and (b) $n = 0.6$. Note only the broad feature indicated by the red arrow at $n = 0.9$ persists at $n = 0.6$.

The two dispersing particle-hole features found here are distinct from a similar feature in stripe models.[47] In such models, the second branch[47] has vanishing weight, whereas in the current theory, both features are of unit weight.

D. Heat conductivity and heat capacity

As shown by Loram *et al.*,[48] the heat capacity in the cuprates in the normal state scales as T^2. Quite generally, a density of states that vanishes linearly with energy, that is, a V-shaped gap, yields a heat capacity that scales quadratically

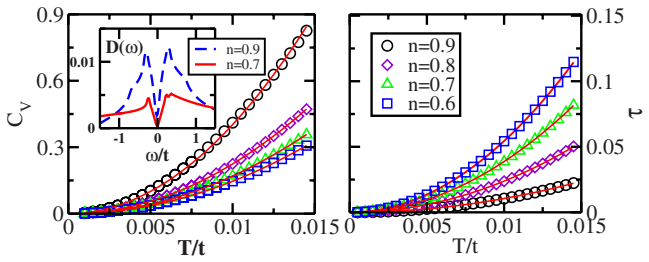

FIG. 9. (Color online) (a) Heat capacity C_V and (b) thermal conductivity τ calculated at $n=0.9$. The solid lines are a fit to T^2. Inset: Density of states for $U=10t$ are evaluated at $n=0.9$ and $n=0.7$, respectively.

with temperature. The coefficient of the T^2 term is determined by the slope of the density of states in the vicinity of the chemical potential. The magnitude of the T^2 term should diminish as the doping increases because the slope of the density of states decreases as the pseudogap closes. As we showed in the previous section, the boson creates a pseudogap. The energy dependence of the gap is shown in the inset of Fig. 9. Quite evident is the linear dependence on energy. The resultant heat capacity shown in Fig. 9(a), calculated via the relationship $C_v=\frac{d\bar{E}}{dt}$, where the internal energy $\bar{E}$ is

$$\bar{E}=\int d\omega D(\omega)\omega f(\omega) \tag{20}$$

and $D(\omega)=\Sigma_{\mathbf{k}}A(\omega,\mathbf{k})$ is the density of states, displays a perfectly quadratic temperature dependence in the doping regime where the pseudogap is present, as is seen experimentally.[48] As it is the boson that underlies the pseudogap, it is the efficient cause of the T^2 dependence of the heat capacity. In our theory, the steeper slope occurs at smaller doping which gives rise to the largest heat capacity at half-filling. This doping dependence of the heat capacity seems to contradict the experimental observations.[48] A key in determining the magnitude of the heat capacity is the spin degrees of freedom. As we have focused entirely on the bosonic degree of freedom and not on the contribution from the spin-spin interaction terms, we have overestimated the kinetic energy. Such terms, though they do not affect the pseudogap found here [from Eq. (6), it is clear that the spin-spin terms renormalize the standard fermionic branch in the lower-Hubbard band, leaving the new state mediated by φ_i untouched], do alter the doping dependence.[42]

Additionally, the thermal conductivity $\tau(T)$ can be calculated using the Kubo formula in noncrossing approximation,

$$\tau(T)=\frac{e}{4k_BT}\sum_{\mathbf{k}}\int\frac{d\omega}{2\pi}(v_{\mathbf{k}}^x)^2\omega^2\left(-\frac{\partial f(\omega)}{\partial\omega}\right)A(\mathbf{k},\omega)^2.$$

The thermal conductivity shown in Fig. 9 scales as T^2 which is identical to that of the heat capacity. However, the system exhibits a larger thermal conductivity as the doping increases, in contrast to the heat capacity which is decreasing as the doping increases. Physically, this signifies that the carriers are more mobile as the doping increases.

E. T-linear resistivity

Over a funnel-shaped region in the T-x plane, the resistivity displays the anomalous linear-T dependence. The standard explanation[49] attributes T-linear resistivity to quantum criticality. However, Phillips and Chamos have recently shown[49] that under three general assumptions, (1) one-parameter scaling, (2) the critical degrees of freedom carry the current, and (3) charge is conserved, the resistivity in the quantum critical regime takes the universal form

$$\sigma(\omega=0)=\frac{Q^2}{\hbar}\Sigma(0)\left(\frac{k_BT}{\hbar c}\right)^{(d-2)/z}. \tag{21}$$

Consequently, T-linear resistivity is obtained (for $d=3$) only if the dynamical exponent satisfies the unphysical constraint $z<0$. The inability of Eq. (21) to lead to a consistent account of T-linear resistivity signifies that either (1) T-linear resistivity is not due to quantum criticality, (2) additional noncritical degrees of freedom are necessarily the charge carriers, or (3) perhaps some new theory of quantum criticality can be constructed in which the single-correlation length hypothesis is relaxed.

We show that the low-energy theory presented here contains elements of both (2) and (3) which lead to T-linear resistivity. The formation of the pseudogap and the divergence of the electrical resistivity are highly suggestive of a bound state between a hole and the charge $2e$ bosonic field, namely, the $\varphi^{\dagger}c_{i\bar{\sigma}}$ particle discussed earlier in the electron operator and the new feature in the dielectric function. Let us assume this state of affairs obtains and the binding energy is E_B. As a bound state, $E_B<0$, where energies are measured relative to the chemical potential. Upon increased hole doping, the chemical potential decreases. Beyond a critical doping, the chemical potential crosses the energy of the bound state. At the critical value of the doping where $E_B=0$, the energy to excite a boson vanishes (as shown in Fig. 10). The critical region is dominated by electron-boson scattering. In metals, it is well known[50] that above the Debye temperature, the resistivity arising from electron-phonon scattering is linear in temperature. In the critical regime, the current mechanism yields a T-linear resistivity for the same reason. Namely, in the critical region, the energy to create a boson vanishes, and hence the resistivity arising from electron-boson scattering should be linear in temperature. This mechanism is robust as it relies solely on the vanishing of the boson energy at criticality and not on the form of the coupling. To the right of the quantum critical point, standard electron-electron interactions dominate and Fermi liquid behavior is obtained. In this scenario, the quantum critical point coincides with the termination of the pseudogap phase or, equivalently, with the unbinding of the bosonic degrees of freedom.

F. Final remarks

We have shown here that (1) T-linear resistivity, (2) high- and low-energy kinks in the electron dispersion, (3) pseudogap phenomena, (4) midinfrared absorption, (5) T^2 heat capacity, and (6) bifurcation of the electron addition spectrum all emerge from the bosonic degree of freedom

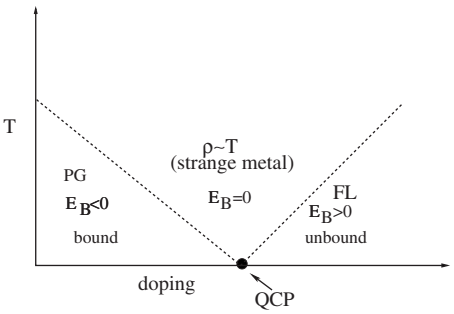

FIG. 10. Proposed phase diagram for the binding of the holes and bosons that results in the formation of the pseudogap phase. Once the binding energy vanishes, the energy to excite a boson vanishes. In the critical regime, the dominant scattering mechanism is still due to the interaction with the boson. T-linear resistivity results anytime $T > \omega_b$, where ω_b is the energy to excite a boson. To the right of the quantum critical regime (QCP), the boson is irrelevant and scattering is dominated by electron-electron interactions, indicative of a Fermi liquid. The QCP signifies the end of the binding of Fermi and bosonic degrees of freedom that results in the pseudogap phase.

which exists in the exact low-energy theory of a doped Mott insulator. All the features found here arise from the charge rather than from the spin dynamics, and hence have nothing to do with the spin-spin interaction of the t-J model. The essential feature of the charge $2e$ boson is that it gives the electron substructure, as is observed experimentally. Further, it does so entirely from a collective mode arising from the strong correlations. No lattice phenomena need be invoked. Consequently, we attribute the anomalies of the normal state of the cuprates to a purely electronic cause which is captured by the physics of the exact low-energy theory of a doped Mott insulator. The key experimental prediction which is sufficient to falsify this theory is the existence of a sharp quasiparticle excitation in the inverse dielectric function. The new quasiparticle represents the collective motion of a double occupancy and a hole, as depicted in Fig. 1, which emerges naturally in the exact low-energy theory as a charge $2e$ boson bound to a hole. The existence of such a quasiparticle underscores the fact that double occupancy at low energy requires a hole in its immediate vicinity. Since this prediction is sharp, experimental falsification of this theory should be straightforward.

ACKNOWLEDGMENTS

This research was supported in part by the NSF DMR-0605769 and NSF under Grant No. PHY05-51164 (T.-P.C. and P.P.). We thank G. A. Sawatzky for insightful discussions and the Kavli Institute of Theoretical Physics, where this paper became finalized, for the hospitality.

[1] For a review, see B. Batlogg, H. Takagi, H. L. Kao, and J. Kwo, in *Electronic Properties of High-T_c Superconductors*, edited by H. Kuzmany, Michael Mehring, and J. Fink (Springer-Verlag, Berlin, 1993), pp. 5–12.

[2] H. Alloul, T. Ohno, and P. Mendels, Phys. Rev. Lett. **63**, 1700 (1989).

[3] M. R. Norman, H. Ding, M. Randeria, J. C. Campuzano, T. Yokoya, T. Takeuchi, T. Takahashi, T. Mochiku, K. Kadowaki, P. Guptasarma, and D. G. Hinks, Nature (London) **392**, 157 (1998); N. P. Armitage *et al.*, Phys. Rev. Lett. **88**, 257001 (2002).

[4] A. Kanigel, M. R. Norman, M. Randeria, U. Chatterjee, S. Souma, A. Kaminski, H. M. Fretwell, S. Rosenkranz, M. Shi, T. Sato, T. Takahashi, Z. Z. Li, H. Raffy, K. Kadowaki, D. Hinks, L. Ozyuzer, and J. C. Campuzano, Nat. Phys. **2**, 447 (2006).

[5] T. Timusk and B. Statt, Rep. Prog. Phys. **62**, 61 (1999).

[6] S. L. Cooper, G. A. Thomas, J. Orenstein, D. H. Rapkine, A. J. Millis, S.-W. Cheong, A. S. Cooper, and Z. Fisk, Phys. Rev. B **41**, 11605 (1990); S. L. Cooper, D. Reznik, A. Kotz, M. A. Karlow, R. Liu, M. V. Klein, W. C. Lee, J. Giapintzakis, D. M. Ginsberg, B. W. Veal, and A. P. Paulikas, *ibid.* **47**, 8233 (1990).

[7] S. Uchida, T. Ido, H. Takagi, T. Arima, Y. Tokura, and S. Tajima, Phys. Rev. B **43**, 7942 (1991).

[8] D. van der Marel, H. J. A. Molegraaf, J. Zaanen, Z. Nussinov, F. Carbone, A. Damascelli, H. Eisaki, M. Greven, P. H. Kes, and M. Li, Nature (London) **425**, 271 (2003).

[9] S. W. Moore, J. M. Graybeal, D. B. Tanner, J. Sarrao, and Z. Fisk, Phys. Rev. B **66**, 060509 (2002).

[10] J. Bouvier, N. Bontemps, M. Gabay, M. Nanot, and F. Queyroux, Phys. Rev. B **45**, 8065 (1992).

[11] Y. S. Lee, Kouji Segawa, Z. Q. Li, W. J. Padilla, M. Dumm, S. V. Dordevic, C. C. Homes, Yoichi Ando, and D. N. Basov, Phys. Rev. B **72**, 054529 (2005).

[12] B. Baskaran, Z. Zou, and P. W. Anderson, Solid State Commun. **63**, 973 (1987).

[13] S. A. Kivelson, D. S. Rokhsar, and J. P. Sethna, Phys. Rev. B **35**, 8865 (1987).

[14] N. Read and B. Chakraborty, Phys. Rev. B **40**, 7133 (1989); N. Read and S. Sachdev, Phys. Rev. Lett. **66**, 1773 (1991).

[15] C. Mudry and E. Fradkin, Phys. Rev. B **49**, 5200 (1994).

[16] T. Senthil and M. P. A. Fisher, Phys. Rev. B **62**, 7850 (2000).

[17] P. A. Lee, N. Nagoasa, and X.-G. Wen, Rev. Mod. Phys. **78**, 17 (2006).

[18] X. G. Wen, Phys. Rev. B **44**, 2664 (1991); **65**, 165113 (2002).

[19] L. Balents and S. Sachdev, Ann. Phys. **322**, 2635 (2007).

[20] B. I. Shraiman and E. D. Siggia, Phys. Rev. Lett. **60**, 740 (1988); **62**, 1564 (1989).

[21] A. H. MacDonald, S. M. Girvin, and D. Yoshioka, Phys. Rev. B **41**, 2565 (1990).

[22] R. B. Laughlin, arXiv:cond-mat/0209269 (unpublished).

[23] E. Altman and A. Auerbach, Phys. Rev. B **65**, 104508 (2002).

[24] P. W. Anderson, P. A. Lee, M. Randeria, T. M. Rice, N. Trivedi, and F. C. Zhan, J. Phys.: Condens. Matter **16**, R755 (2004).

[25] T. C. Ribeiro and X.-G. Wen, Phys. Rev. Lett. **95**, 057001 (2005).

[26] Z.-Yu Weng, Int. J. Mod. Phys. B **21**, 773 (2007).

[27] S. E. Barnes, J. Phys. F: Met. Phys. **6**, 1375 (1976); **7**, 2637 (1977).
[28] P. Coleman, Phys. Rev. B **29**, 3035 (1984).
[29] G. Kotliar and A. E. Ruckenstein, Phys. Rev. Lett. **57**, 1362 (1986).
[30] R. G. Leigh, P. Phillips, and T.-P. Choy, Phys. Rev. Lett. **99**, 046404 (2007).
[31] T.-P. Choy, R. G. Leigh, P. Phillips, and P. D. Powell, Phys. Rev. B **77**, 014512 (2008).
[32] H. Eskes, A. M. Oles, M. B. J. Meinders, and W. Stephan, Phys. Rev. B **50**, 17980 (1994).
[33] A. L. Chernyshev, D. Galanakis, P. Phillips, A. V. Rozhkov, and A.-M. S. Tremblay, Phys. Rev. B **70**, 235111 (2004).
[34] J.-Y. P. Delannoy, M. J. P. Gingras, P. C. W. Holdsworth, and A.-M. S. Tremblay, Phys. Rev. B **72**, 115114 (2005).
[35] P. Phillips, T.-P. Choy, and R. G. Leigh, arXiv:0802.3405 (unpublished).
[36] A. Lanzara, P. V. Bogdanov, X. J. Zhou, S. A. Kellar, D. L. Feng, E. D. Lu, T. Yoshida, H. Eisaki, A. Fujimori, K. Kishio, J.-I. Shimoyama, T. Noda, S. Uchida, Z. Hussain, and Z.-X. Shen, Nature (London) **412**, 510 (2001).
[37] J. Graf, G.-H. Gweon, K. McElroy, S. Y. Zhou, C. Jozwiak, E. Rotenberg, A. Bill, T. Sasagawa, H. Eisaki, S. Uchida, H. Takagi, D.-H. Lee, and A. Lanzara, Phys. Rev. Lett. **98**, 067004 (2007).
[38] M. B. J. Meinders, H. Eskes, and G. A. Sawatzky, Phys. Rev. B **48**, 3916 (1993).
[39] T.-P. Choy and P. Phillips, Phys. Rev. Lett. **95**, 196405 (2005).
[40] T. D. Stanescu, P. Phillips, and T.-P. Choy, Phys. Rev. B **75**, 104503 (2007).
[41] A. Comanac, L. de Medici, M. Capone, and A. J. Millis, arXiv:0712.2392 (unpublished).
[42] M. M. Zemljič and P. Prelovšek, Phys. Rev. B **72**, 075108 (2005).
[43] K. Haule and G. Kotliar, Europhys. Lett. **77**, 27007 (2007).
[44] J. Hwant, T. Timusk, and G. D. Gu, J. Phys.: Condens. Matter **19**, 125208 (2007).
[45] Y. Onose, Y. Taguchi, K. Ishizaka, and Y. Tokura, Phys. Rev. B **69**, 024504 (2004).
[46] A. Lucarelli, S. Lupi, M. Ortolani, P. Calvani, P. Maselli, M. Capizzi, P. Giura, H. Eisaki, N. Kikugawa, T. Fujita, M. Fujita, and K. Yamada, Phys. Rev. Lett. **90**, 037002 (2003).
[47] V. Cvetkovic, Z. Nussinov, S. Mukhin, and J. Zaanen, Europhys. Lett. **81**, 27001 (2007).
[48] J. W. Loram, J. Luo, J. R. Cooper, W. Y. Liang, and J. L. Tallon, J. Phys. Chem. Solids **62**, 59 (2001).
[49] P. Phillips and C. Chamon, Phys. Rev. Lett. **95**, 107002 (2005).
[50] J. Bass, W. P. Pratt, and P. A. Schroeder, Rev. Mod. Phys. **62**, 645 (1990).